Agriculture, Ecosystems and Environment 325 (2022) 107721

Contents lists available at ScienceDirect

Agriculture, Ecosystems and Environment

journal homepage: www.elsevier.com/locate/agee

Effects of deforestation and afforestation on water availability for dry bean production in Haiti

R. Mompremier [a], Y. Her [b,*], G. Hoogenboom [a,c], J. Song [b]

[a] Department of Agricultural and Biological Engineering, Institute of Food and Agricultural Sciences, University of Florida, Gainesville, USA
[b] Department of Agricultural and Biological Engineering / Tropical Research and Education Center, Institute of Food and Agricultural Sciences, University of Florida, Homestead, USA
[c] Institute for Sustainable Food Systems, University of Florida, Gainesville, USA

ARTICLE INFO

Keywords:
Watershed modeling
Streamflow monitoring
Irrigation
Land use changes
SWAT
DSSAT

ABSTRACT

Haitian watersheds suffer from a lack of environmental management and the absence of conservation practices, which impairs natural resources and agricultural productivity. This is aggravated by harvesting trees to compensate for reduced crop production and income. Deforestation can further deteriorate the natural and agricultural systems by increasing the temporal variability of water availability, often realized in the forms of floods and droughts. The goal of this study was to determine the effects of both deforestation and afforestation on water resources and agricultural productivity. We selected the Courjolle River watershed and its downstream irrigation districts because they represent the linkage between the upstream forest and downstream agricultural areas. Watershed hydrology and dry bean growth were simulated with the Soil and Water Assessment Tool (SWAT) model and the CSM-CROPGRO–Dry bean model of the Decision Support System for Agrotechnology Transfer (DSSAT). The parameters for both models were calibrated to streamflow and dry bean growth measurements that were made in the study areas. Deforestation and afforestation scenarios were developed based on an understanding of the local landscape. The modeling experiment showed that deforestation could decrease water availability and stability, causing a decrease in dry bean production, while afforestation had the opposite effect. An increase of the afforested areas from 25% to 100% of the watershed increased the streamflow by 2–7%, compared to the current land cover, during dry periods. On the other hand, an increase in deforested areas decreased the amount of available water for downstream agricultural areas by 6–24%. Potential changes in the water availability due to the land cover changes then affected the yield of dry bean grown in the downstream irrigation areas, from −42–24% under the deforestation and afforestation scenarios. The study demonstrated how improved hydrologic stability due to an increase in tree cover could promote agricultural production. It also showed that afforestation could be an effective way to manage both the natural and agricultural resources in Haiti, improving the environmental sustainability of the watershed and the economic sustainability of local smallholder farmers.

1. Introduction

In Haiti, forests first started being cleared during the colonial period from 1697 to 1804 to grow cash crops such as coffee and sugar cane, and deforestation has continued to the present day (Runge and White, 1994; Tarter et al., 2017; Hedges et al., 2018). The demand for fuelwood and charcoal also has contributed substantially to forest degradation in addition to crop production (Ghilardi et al., 2018). Deforestation and urbanization are known to increase peak flows and flood risk during the rainy season and decrease baseflow during the dry season (Sahin and Hall, 1996; Bruijnzeel, 2004; Marhaento et al., 2017). Although deforestation is believed to affect Haitian water resources and agriculture negatively, the impacts have not been quantified in order to guide natural resources management planning and practices (Wampler et al., 2019).

Land management plays an essential role in the protection of soil and water resources and, thus, helps to improve sustainability (Nikolaidis et al., 2013; Abdelwahab et al., 2014, 2018; Bisantino et al., 2015). Many considerations are made when developing natural resource conservation plans, such as socio-economic, human-institutional, and

* Corresponding author.
E-mail address: yher@ufl.edu (Y. Her).

https://doi.org/10.1016/j.agee.2021.107721
Received 27 January 2021; Received in revised form 1 October 2021; Accepted 13 October 2021

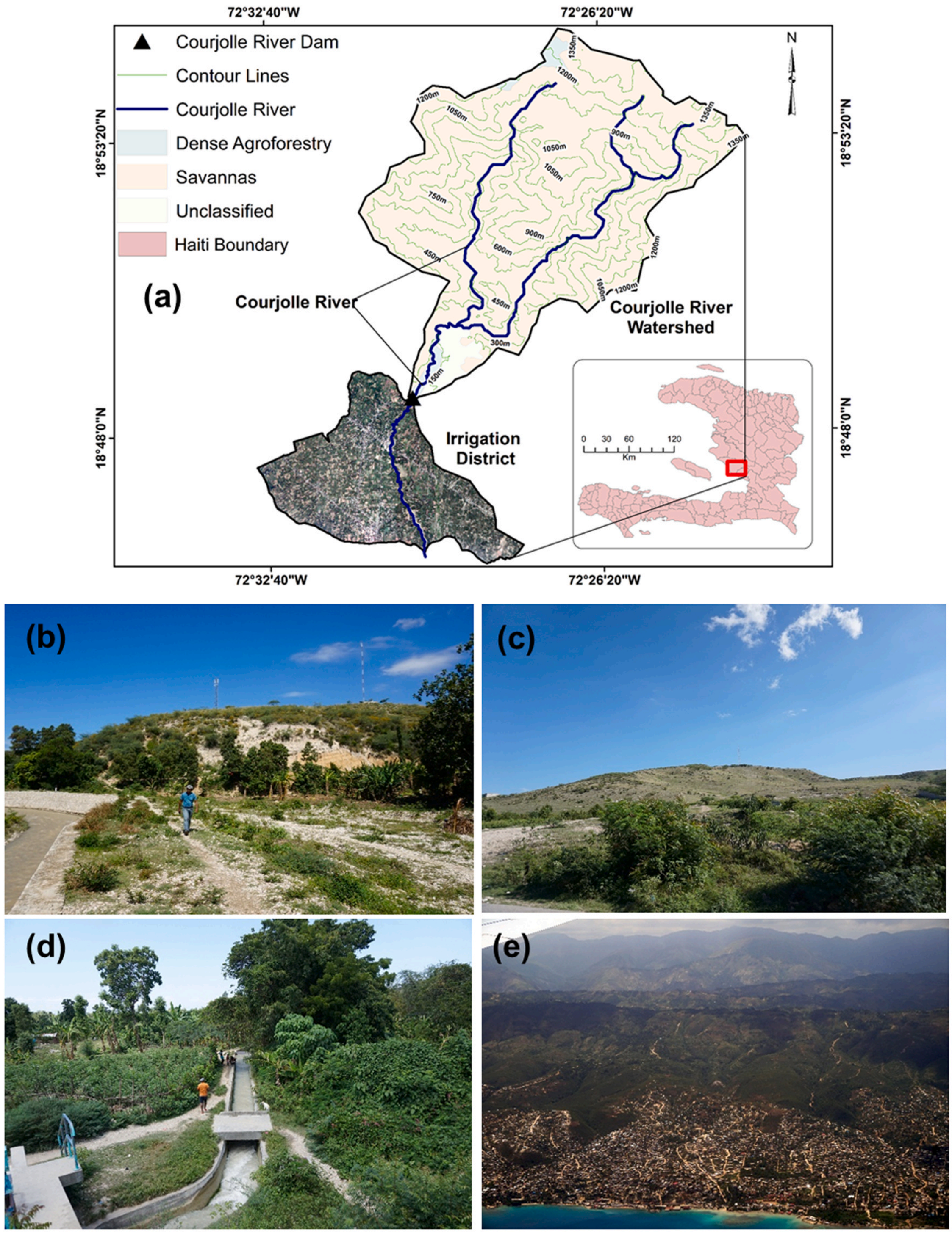

Fig. 1. Location of the study area that includes the Courjolle River Watershed (CRW) and dry bean irrigation area (a), the (upstream) Courjolle River watershed (b), the savanna landscape of the study area (c), the canal in the (downstream) irrigation district (d), and the typical landscape (forest-savanna-agriculture/urban) of coastal areas in Haiti (from an airplane) (e).

biophysical inter-relationships among soil, water, and land use and the connection between upland and downstream areas. However, until now, this has not been the focus for watershed management in Haiti (Ffolliott et al., 2002). It has been reported that approximately 30% of the land in Haiti has been irreversibly degraded (Gardi et al., 2014). It is, therefore, critical to develop and implement effective management plans and practices to end land degradation and restore hydrological conditions and processes for improved sustainability of Haitian agriculture and natural resources.

Streamflow as the main source of water for agricultural irrigation is controlled by the landscape, including land cover, topography, and soil, as well as rainfall and its spatio-temporal variability (CNSA/MARND, 2013; Molnar et al., 2015; Fews Net and USAID, 2018). Studies have shown how the streamflow responds to changes in land use and climate (Neupane et al., 2015; Belmar et al., 2016; Anaba et al., 2017; Marhaento et al., 2017). Extensive human-induced land use changes are a major global environmental issue, affecting hydrologic processes such as rainfall interception, evapotranspiration, and surface soil hydraulic

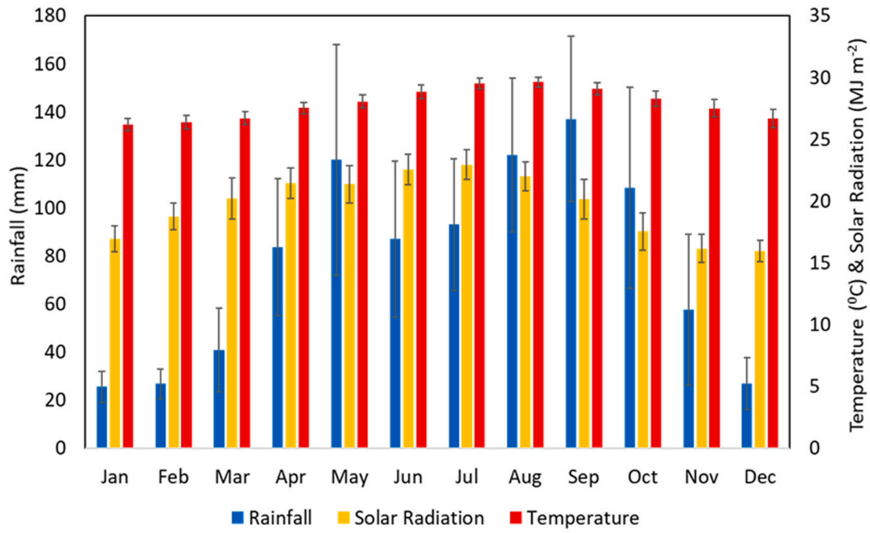

Fig. 2. Long-term average monthly total rainfall (CHIRPS; 1981 – 2017), and solar radiation, and temperature (NASA-POWER; 1984 – 2018) data for Arcahaie, Haiti. The error bars represent the variability.

conductivity and, thus, water availability and the overall water balance (He et al., 2008; Germer et al., 2009; Scheffler et al., 2011; Muñoz-Villers and McDonnell, 2013; Yan et al., 2013; Nepal et al., 2014). The impact of land use changes on streamflow can be significant, especially for tropical areas such as Haiti that have greater energy inputs and a faster rate of natural processes (Wohl et al., 2012).

Mathematical models are commonly used as a tool to examine the effect of land use and management practices on water resources (Naef et al., 2002; Thanapakpawin et al., 2007; Huisman et al., 2009). There are many hydrologic models available to represent the hydrological processes of a watershed, and the Soil and Water Assessment Tool (SWAT) is one of the models that has been used widely, especially in developing countries, presumably due to its relatively simple simulation concept and mechanism, its comprehensive supporting documents, various pre- and post-processing tools, and continuous model maintenance and updates (Arnold et al., 1998, 2012; Gassman et al., 2007; Her, and Heatwole, 2016; Her et al., 2017). The SWAT model divides a watershed by its subbasins, land use and cover, soils, and slopes, which allows for a proper representation of the spatial variation of the landscape components and section for hydrologic modeling. The model has been used extensively to assess the effects of land use and management changes on watershed responses, including streamflow (Van Liew et al., 2007; Schilling et al., 2008; Neupane et al., 2015; Giri et al., 2016; Her et al., 2016).

Crop models can help investigate the responses of crops to management practices and changes in the environment. The Decision Support System for Agrotechnology Transfer (DSSAT) crop models (Hoogenboom et al., 2019a, 2019b; Jones et al., 2003) have been used extensively in the crop modeling community to address various questions related to yield response to management practices including irrigation (Ben Nouna et al., 2000; Heinemann et al., 2000; Hundal and Prabhjyot-Kaur, 1997; MacRobert and Savage, 1998; Steele et al., 2000). Nicolas et al. (2020) applied the DSSAT tool to assess the impact of climate change on rice production in the Artibonite Valley of Haiti and found that the average annual rice yield might decrease in the future. Malik et al. (2020) coupled two models, DSSAT and SWAT, to assess the efficacy of best management practices related to nitrogen application and irrigation optimization. Malik et al. (2019) also used DSSAT to find the optimal management practices that can minimize the application rates of irrigation water and fertilizers without significant reduction in yield. Mompremier et al. (2021) found that shifting crop (dry bean) growing season earlier can better secure irrigation water and improve agricultural productivity using DSSAT and hydrological monitoring. Other studies applied the DSSAT to evaluate the effects of irrigation levels on soil moisture availability for maize (Dokoohaki et al., 2017), to investigate the response of maize and soybean crops to water-limited conditions by applying water available at specific crop growth stages (Lopez et al., 2017) to optimize nitrogen application at field level (Jeong et al., 2014)) and to investigate the effects of water management on crop production (Attia et al., 2016)).

Governmental and non-governmental (NGOs) institutes have been implementing debates and actions in favor of the reforestation of the mountainous areas in Haiti (Widmer et al., 2018). Several studies have investigated the relationship between deforestation, environmental quality, fuelwood consumption in Haiti, and the perception of farmers toward forest conservation (McClintock, 2003; Dolisca et al., 2006a, 2006b, 2007, 2009; Tarter, 2016; Ghilardi et al., 2018). They found that deforestation was closely linked to the limited source of energy in Haiti. Wood is commonly used to produce charcoal as the main source of energy for cooking food and baking bread. Churches et al. (2014) evaluated the spatio-temporal changes of Haiti's forest coverage using Landsat imagery, and Balogun Mohammed et al. (2018) assessed alternative bioenergy crops to replace trees as feedstock for charcoal production. Although deforestation is expected to have a negative effect on natural resources and agriculture, the impacts have not been quantified for Haiti, and the connection until now has not been explored.

The goal of this study was to assess how forest land use change can affect watershed hydrology and agriculture. The specific objectives include investigating the direct effects of afforestation and deforestation on streamflow and their subsequent impacts on irrigation water availability and crop production. This paper describes the clear linkage between land use, hydrology, and agriculture and discusses the implications and limitations of this work.

2. Methods and materials

2.1. Study area

This study focused on the Coujolle River Watershed (CRW) located in the Arcahaie region of Haiti. This watershed represents a typical agricultural landscape, with upstream mountainous watersheds connected to downstream low-lying irrigation areas (Fig. 1). This watershed drains water from 80 km^2, and it is dominated by savanna (97%) (CNIGS, 2008). The National Aeronautics and Space Administration (NASA) global Shuttle Radar Topography Mission (SRTM) data show that the elevation of the watershed ranges from 100 to 1498 m above mean sea

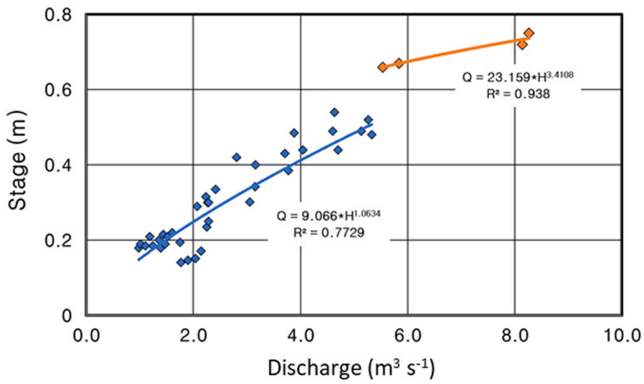

Fig. 3. Rating curve developed from the Courjolle River flow monitoring.

level (USGS, 2019). The FAO Digital Soil Map of the World (DSMW) indicates that the study area encompasses different soil types, including silty clay loam, sandy loam, and clay loam (FAO-UNESCO, 2003). The average annual rainfall between 1981 and 2017 obtained from the Climate Hazards Group InfraRed Precipitation with Station data (CHIRPS) was 928 mm (Funk et al., 2015; Dinku et al., 2018). The monthly average air temperature between 1984 and 2018 obtained from NASA POWER ranged from 26.2 °C for August (warmest) to 29.6 °C for January (coolest) (Fig. 2) (Pandey et al., 2016; Lopez et al., 2017; Stackhouse et al., 2018; Maldonado et al., 2019). The CRW is critical in providing water for domestic use and agricultural production in its downstream areas. The Arcahaie region is known for its capacity for producing dry bean and plantain in Haiti (RGA/MARNDR, CNIGS, FAO, and European Union, 2012). However, the local farmers are challenged to find sufficient water for irrigation during the dry season (MARNDR, 2012).

2.2. Streamflow monitoring

Streamflow level was recorded at the outlet of CRW every minute from August 2018 to April 2019. Once a week, the water level was read on a staff, and the cross-section and the flow velocity were measured. From the records, a rating curve was constructed for the outlet, and then the flow discharge was calculated from the water level (Fig. 3).

The calculated streamflow discharge was analyzed to characterize the pattern of the flow variation in reaction to rainfall events and investigate how the pattern (or flow regime) responds to land use change scenarios (Poff et al., 1997; Baker et al., 2004). In this study, the Richards-Baker (R-B) flashiness index was used to characterize the streamflow regime and responsiveness to rainfall events at a daily scale (Baker et al., 2004; Eq. (1)).

$$R-B \quad flashiness \quad index = \frac{\sum_{i=1}^{n}|q_i - q_{i-1}|}{\sum_{i=1}^{n} q_i} \tag{1}$$

where q is daily flow, i is time (day), and n is the number of days. The R-B flashiness index quantifies the degree of oscillations in daily flow compared to total flow for a given period. Thus, daily streamflow with relatively high temporal variations will yield a greater R-B flashness index value. On the other hand, relatively stable streamflow will result in a smaller index value. Baker et al. (2004) found the index is negatively correlated to baseflow and watershed areas and suggested its use for identifying changes in flow regimes in response to changes in land cover and management practices.

Table 1
Input data for watershed modeling with SWAT.

Data	Source	Format	Scale or Resolution	Date
DEM[a]	USGS	Raster	30-m resolution	2000
LULC[b]	CNIGS[c]	Polygon	1:100,000	1998
Soil	FAO-UNESCO	Raster	1:5000,000	2003
Weather	UHM	Tabular data	–	2014–2019
	NASA	Raster	0.5° × 0.5°	2014–2019
Streamflow	Measured	Tabular data	–	2018–2019

[a] DEM: Digital Elevation Model.
[b] LULC: Land Use and Land Cover.
[c] CNIGS: Centre National de de l'Information Geo-Spatial.

2.3. Watershed model preparation

The hydrological characteristics and processes of the CRW were mathematically described using the SWAT model (Arnold et al., 1998), which was also used to represent deforestation and afforestation scenarios and simulate the impact on the streamflow responses of the CRW. Previous studies have shown the capacity of SWAT as a tool to simulate hydrological watershed responses to changes in land use such as tree coverage (Sun et al., 2005; Neupane et al., 2015; Marhaento et al., 2017).

For the SWAT modeling component, topography data in raster format with a 30-m resolution (SRTM 1-arc-Second Global) were obtained from the United States Geological Survey (USGS) (accessible at https://earthexplorer.usgs.gov/) (Table 1). The soil information was retrieved from the Food and Agricultural Organization – United Nations Educational, Scientific and Cultural Organization (FAO – UNESCO) soil database (FAO-UNESCO, 2003). The most recent (1998) land cover data were obtained from the Haitian government (CNIGS) (CNIGS, 2008). The closest local weather station is located at an approximate distance of 10 km from the CRW, and it is managed by the Haitian Unité Hydro Météorologie (UHM). The UHM provided the rainfall data from 2016, when the station started collecting rainfall data, to 2019. The solar radiation, temperature, wind speed, and relative humidity were downloaded from the NASA POWER portal for the same period (2014–2019) (accessible at https://power.larc.nasa.gov/data-access-viewer/) for model calibration and scenario analysis (Pandey et al., 2016; Lopez et al., 2017; Maldonado et al., 2019). Missing rainfall data of UHM were filled by replacing values from other sources (CHIRPS; Funk et al., 2015).

The CRW land cover is characterized by savanna (97%) and dense agroforestry system (2%) (CNIGS, 2008). The compiled landscape and weather information was used as input data for the SWAT model, which was set up with 25 subbasins and 212 hydrological response units (HRUs) with a stream initiation threshold of 1.5 km^2 and HRU threshold of 5% (land use) – 5% (soil) – 5% (slope) (Her et al., 2015) (Fig. 4). The dominant land cover, i.e., savanna, was represented by trees/shrubs in poor condition where "forest litter, small trees, and brush are destroyed by heavy grazing or regular burning" (Haan et al., 1994; Neitsch et al., 2011).

The SWAT model was calibrated and evaluated to the daily streamflow that was measured at the outlet of the watershed from August 2018 to April 2019, and the model was then used to simulate the runoff processes in response to land cover change scenarios. Based on an understanding of the hydrological process of the study areas, literature,

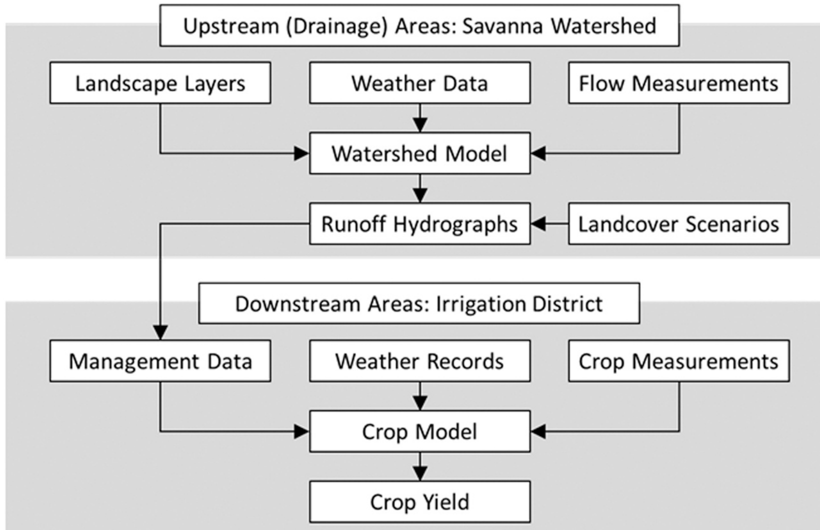

Fig. 4. Overall procedures for determining the effect of runoff on dry bean yield for different forestation scenarios.

Table 2
SWAT parameters for streamflow calibration.

Parameters	Description	Variation Method	Ranges	
			Min	Max
SOL_AWC	Available water capacity of the soil layer (mm/mm)	r[a]	-0.25	0.25
SOL_K	Saturated hydraulic conductivity (mm/hr)	r	0.25	0.25
SLSUBBSN	Average slope length.	v[b]	10	150
HRU_SLP	Average slope steepness	r	-0.5	1
CN2	SCS runoff curve number	r	-0.25	0.25
SURLAG	Surface runoff lag time	v	0.05	24
GW_REVAP	Groundwater evaporation coefficient	v	0.02	0.2
ALPHA_BF	Baseflow alpha factor (days)	v	0	1
GW_DELAY	Groundwater delay time (day)	v	0	500
REVAPMN	Depth of water for evaporation (mm)	v	0	500
GWQMN	Depth of water for return flow (mm)	v	0	5000
RCHRG_DP	Deep aquifer percolation fraction	v	0	1
CH_K2	Effective hydraulic conductivity in main channel alluvium (mm/hr)	v	0.01	150
OV_N	Manning's "n" value for overland flow	v	0.01	30
ESCO	Soil evaporation compensation factor	v	0.01	1
EPCO	Plant uptake compensation factor	v	0.01	1

[a] r: means a relative change in the parameter where the current value is multiplied by one plus a factor in the given range after each iteration during the calibration process.
[b] v: means a substitution of a parameter by a value from the given range after each iteration during the calibration process.

and expert judgment, sixteen key parameters were selected for calibration (Table 2; Arnold et al., 2012). The state variables (e.g., the total amount of water in the soil profile) of the model were stabilized for a simulation period from January 2014 to August 2018. This study was able to obtain streamflow observations for nine months, but the flow monitoring could not expand beyond that point due to limited access to the study areas and security management issues. Thus, a differential split-sample test was implemented to make maximum use of the monitoring data and improve the representativity of a calibrated parameter with a limited amount of data. The streamflow monitoring data were split into four periods based on the hydrological regimes (two wet and two dry periods): Wet1 (August 22, 2018 to October 11, 2018), Wet2 (October 12, 2018 to December 1, 2018), Dry1 (December 2, 2018 to February 11, 2019), and Dry2 (February 13, 2019 to April 23, 2019). Then, a differential split-sample test was performed to calibrate and evaluate the model using the two pairs of sub-periods' streamflow observations: Wet1-Dry2 and Wet2-Dry1. For instance, when the first wet period (Wet1) and the second dry period (Dry2) were used to calibrate the parameters in the first calibration trial (FCT), the second wet period (Wet2) and the first dry period (Dry1) were employed to evaluate the calibrated model.

The model parameter space was explored using the Latin hypercube sampling approach (McKay et al., 1979, 2000; Ye, 1998) from the Sequential Uncertainty Fitting version 2 incorporated in the SWAT Calibration and Uncertainty Procedure (SWAT-CUP) tool. In each of the calibration trials, a total of 4000 parameter sets were sampled and evaluated to find one that provided the best accuracy statistics (Marhaento et al., 2017). The Nash–Sutcliffe Efficiency (Nash and Sutcliffe, 1970) and Kling-Gupta Efficiency (Gupta et al., 2009) were selected as objective functions, which were then maximized in the calibration.

$$NSE = 1 - \frac{\sum_{i=1}^{n}\left(Q_{obs(i)} - Q_{sim(i)}\right)^2}{\sum_{i=1}^{n}\left(Q_{obs(i)} - \overline{Q}_{obs}\right)^2} \tag{2}$$

where, $Q_{obs(i)}$ is the ith observed daily discharge data, $Q_{sim(i)}$ is the ith simulated daily discharge data, and $\overline{Q}_{obs}$ is the mean observed data, and n is the total number of observed data.

$$KGE = 1 - \left((r-1)^2 + (\alpha-1)^2 + (\beta-1)^2\right)^{1/2} \tag{3}$$

where $\alpha = \frac{\sigma_s}{\sigma_m}$, $\beta = \frac{\mu_s}{\mu_m}$, and r is the linear regression coefficient between simulated and measured discharge, μ_s and μ_m are the means of the simulated and measured data, and σ_s and σ_m are the standard deviation of simulated and measured data, respectively. The performance of a

Table 3
Land use change scenarios.

Land Cover Type Scenarios	Spatial Distribution Scenarios			
	25%	50%	75%	100%
Deforestation	D25[a]	D50	D75	D100
Afforestation	A25[b]	A50	A75	A100

[a] D25, D50, D75, and D100: Upstream watershed with 25%, 50%, 75%, and 100% deforestation.
[b] A25, A50, A75, and A100: Upstream watershed with 25%, 50%, 75%, and 100% afforestation.

calibrated model was further evaluated using other performance statistics such as coefficient of determination (r^2) and percent bias (PBIAS) (Ritter and Muñoz-Carpena, 2013; Abbaspour et al., 2015). A generic model evaluation procedure, FITEVAL, was used to investigate the accuracy in detail (Ritter and Muñoz-Carpena, 2013; Harmel et al., 2018). In this study, NSE equal to or greater than 0.5 and PBIAS smaller than ±15% were regarded acceptable (Moriasi et al., 2015; Harmel et al., 2018).

2.4. Crop model preparation

Local farmers use supplemental irrigation to produce dry bean in the downstream areas of the CRW, with the streamflow discharge of CRW as the main source for water (Fig. 1). The CSM–CROPGRO–Drybean model (Hoogenboom et al., 1992, 1994) of the Decision Support System for Agrotechnology Transfer (DSSAT) (Hoogenboom et al., 2019a, 2019b; Jones et al., 2003) was used to mathematically represent the dry bean physiological processes (Mompremier et al., 2021). Rainfall data obtained from different sources, including NASA-POWER, CHIRPS, and local weather stations of UHM, were combined to create a single time-series as input for the crop model. Soil data used for the crop model simulations were compiled from a local soil survey conducted by Jeune (2015) (Mompremier et al., 2021). Three years of crop management data, including anthesis, physiological maturity, and yield (Raphael Colbert, personal communication), were used for calibration and evaluation of the CSM–CROPGRO–Drybean model (Mompremier et al., 2021). The model was then used to simulate the dry bean yield responses to the different watershed land cover (deforestation and afforestation) scenarios regarding the amount of water that can be provided. In the study areas, farmers grow dry bean from December to March, and the recent data sets received from the Ministry of Agriculture of Haiti for 2015–2016 and 2016–2017 showed that most of the dry bean fields are planted around December 15. Since the focus of the study is to quantify the response of dry bean yield to the variation in water availability (or deficit), we assumed that fertilizer was not limiting and that pests, diseases, and weeds were properly controlled.

2.5. Scenarios analysis

The effects of afforestation and deforestation on water resources in the CRW were evaluated by comparing the simulated total water yield, direct runoff, and baseflow based on the calibrated SWAT model. Then, the impact on dry bean yield was assessed using the CSM-CROPGRO-Drybean model to which the available water simulated with the watershed model was provided as input data. This modeling experiment that loosely coupled two different models for the simulation of hydrology and crop growth (Siad et al., 2019) was expected to enable us to explicitly investigate the linkage between the upstream savanna watershed and downstream agricultural areas.

The current land cover condition, where 97% of the drainage areas of CRW were covered by savanna, was regarded as the baseline in the scenario analysis. Two different land covers and four spatial distributions were combined to create eight land use change scenarios (Table 3

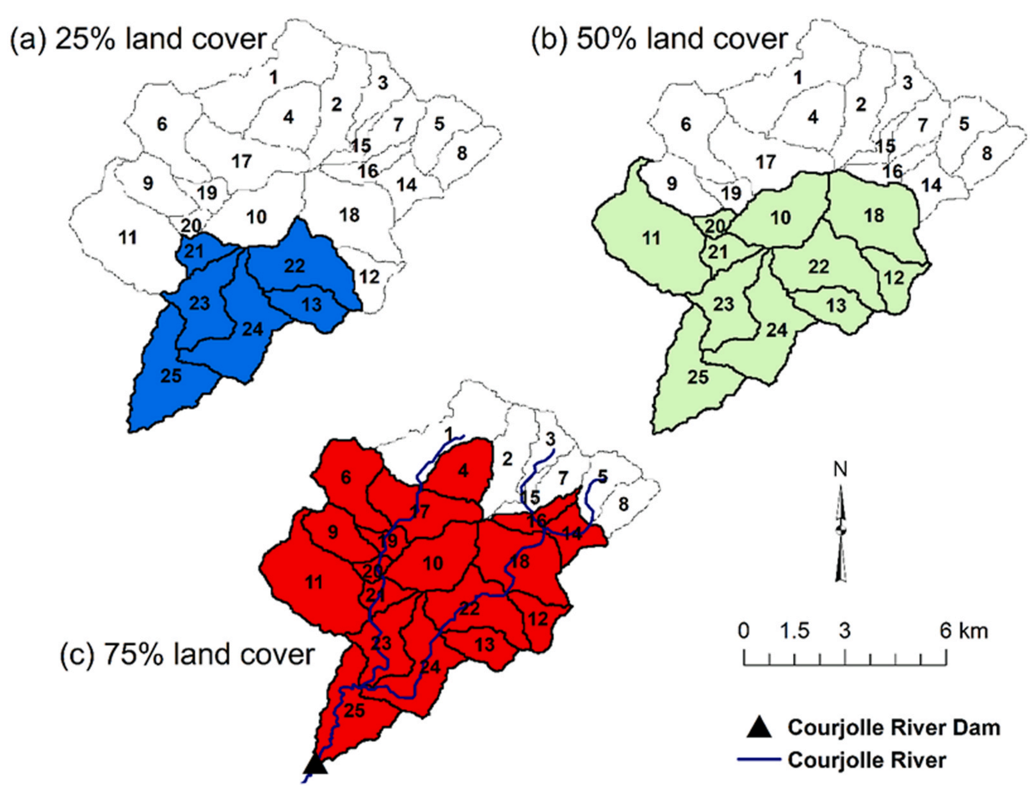

Fig. 5. Spatial distribution of the subbasins in the CRW.

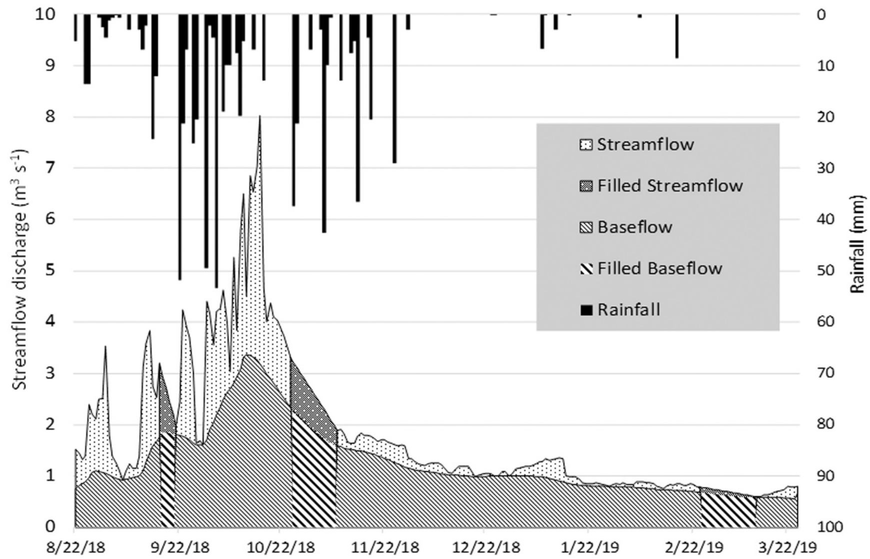

Fig. 6. Streamflow observed at the outlet of the CRW from August 2018 to March 2019. The baseflow was separated from the total runoff using the BFlow method; precipitation was recorded at a local weather station close to the study areas.

Table 4
Final calibrated watershed model parameters using NSE and Kling-Gupta Efficiency (KGE) as the objective functions.

Parameters[a]	Fitted Values (NSE[b])	Fitted Values (KGE[c])	Value Ranges (NSE)		Value Ranges (KGE)	
			Min	Max	Min	Max
GW_DELAY	18.2	17.3	7.00	85.8	0.000	79.0
RCHRG_DP	0.200	0.055	0.080	0.482	0.027	0.313
GWQMN	175	125	0.000	903	0.000	780
GW_REVAP	0.026	0.207	0.023	0.070	0.164	0.217
CN2	-0.247	-0.249	-0.250	-0.159	-0.250	-0.133
SLSUBBSN	95.1	92.0	92.1	131	48.8	104
SURLAG	13.1	9.73	11.9	16.3	9.34	17.3
SOL_AWC	-0.142	0.109	-0.144	-0.050	0.064	0.209
HRU_SLP	0.073	0.717	-0.044	0.239	0.410	0.805
SOL_K	-0.173	0.003	-0.181	-0.043	-0.088	0.067
CH_K2	71.5	72.6	62.7	97.6	43.6	85.3
ALPHA_BF	0.561	0.601	0.555	0.829	0.414	0.643
OV_N	28.4	28.8	24.6	30.0	24.9	30.0
ESCO	0.219	0.707	0.133	0.298	0.654	0.858
EPCO	0.274	0.536	0.116	0.571	0.361	0.711
REVAPMN	105	346	2.00	115	302	434

[a] GW_DELAY: groundwater delay (day), RCHRG_DP: groundwater recharge to the deep aquifer, GWQMN: depth of water for return flow (mm), GW_REVAP: groundwater evaporation coefficient, CN2: curve number, SLSUBBSN: average slope length, SURLAG: surface runoff lag coefficient, SOL_AWC: available water capacity of the soil layer (mm/mm), HRU_SLP: Average slope steepness, SOL_K: Saturated hydraulic conductivity (mm/hr), CH_K2: Effective hydraulic conductivity in main channel alluvium (mm/hr), ALPHA_BF: Baseflow alpha factor, OV_N: Manning's "n" value for overland flow, ESCO: Soil evaporation compensation factor, EPCO: Plant uptake compensation factor, REVAPMN: Depth of water for evaporation.
[b] NSE: Nash-Sutcliffe model Efficiency coefficient.
[c] KGE: Kling-Gupta Efficiency.

and Fig. 4). For instance, an afforestation scenario, so-called a condition "better" than the current, was represented by replacing the savanna with "woods in good condition" where "woods are protected from grazing, and litter and brush adequately cover the soil" in the SWAT modeling (Haan et al., 1994; Neitsch et al., 2011). On the other hand, a deforestation scenario, a condition "worse" than the present land cover (savanna), was described with a "pasture, grassland, or range in a poor condition" where "ground cover less than 50% or heavily grazed with no mulch" in the modeling (Haan et al., 1994; Neitsch et al., 2011).

The simulation period from January 1, 2017 to December 31, 2018 was determined according to the availability of local weather station data, which were obtained from a local weather station managed by the Haitian government. The missing data were replaced with daily data from CHIRPS. Since dry bean is grown from mid-December to the end of March, the water yield simulated with SWAT from December 15, 2017 (dry bean planting date in the district) to March 31, 2018 (end of the dry bean season) was used to estimate the amount of water available for irrigation in the scenario analysis.

The spatial distributions of land cover changes were determined, assuming that the changes, either afforestation or deforestation, start at subbasins close to residential areas in the watershed (Figs. 1 and 5). In the study area, most of the population lives close to their farms that are located downstream of the CRW outlet or dam. In the scenario analysis, thus, subbasins closer to the outlet were assumed to first experience the land cover changes. For instance, the subbasins #13, #21 to #25, whose summed savanna areas correspond to 25% of the total savanna areas of

Table 5
Evaluation of SWAT model performance.

Performance Statistics	First Calibration Trial (FCT)			
	NSE[a] as Objective Function		KGE[b] as Objective Function	
	Calibration	Evaluation	Calibration	Evaluation
NSE	0.67	0.65	0.56	0.63
R^2	0.69	0.65	0.63	0.68
PBIAS[c] (%)	11.9	-1.1	4.5	-7.7
Performance Statistics	Second Calibration Trial (SCT)			
	NSE as Objective Function		KGE as Objective Function	
	Calibration	Evaluation	Calibration	Evaluation
NSE	0.69	0.62	0.65	0.57
R^2	0.69	0.67	0.69	0.58
PBIAS (%)	-3.5	-6.2	0.2	4.0

First Calibration Trial (FCT) was conducted using streamflow observations made in the W2 (second wet) and D1 (first dry) periods for calibration and the W1 and D2 periods for evaluation.
Second Calibration Trial (SCT) was conducted using streamflow observations made in the W1 (first wet) and D2 (second dry) periods for calibration and the W2 and D1 periods for evaluation.
[a] NSE: Nasch and Sutcliffe Efficiency,
[b] KGE: Kling-Gupta efficiency,
[c] PBIAS: Percentage of bias.

the CRW, were selected to represent the 25% land use chance scenario (Fig. 5 and Table 3). The 50% scenario additionally includes the subbasins #10, #11, #12, #18, and #20, and the subbasins #4, #6, #9, #14, #16, #17, and #19 were newly added to the 50% scenario to develop the 75% scenario.

3. Results

3.1. Streamflow and baseflow separation

The streamflow discharge of the CRW showed large temporal variations within the monitoring period from August 2018 to April 2019 (Fig. 6). The average flow was 1.7 $m^3 s^{-1}$ with a standard deviation of 1.3 $m^3 s^{-1}$ and a peak flow of 8 $m^3 s^{-1}$ on October 16, 2018. A baseflow separation implemented using the BFlow model showed that baseflow contributes 70% of the streamflow (Arnold et al., 1995; Arnold and Allen, 1999). The R-B flashiness indices that were calculated (0.12) for the streamflow confirmed that the baseflow was the principal source of surface water for the dry bean growing season (Mompremier et al., 2021).

3.2. Watershed model calibration and evaluation

In the sensitivity analysis, GW_DELAY (groundwater delay) was identified as the most critical parameter, and it was followed by RCHARG_DP (groundwater recharge to deep aquifer), GWQMN (depth of water for return flow), GW_REVAP (groundwater evaporation coefficient), CN2 (curve number), SLSUBBSN (average slope length), SURLAG (surface runoff lag coefficient), and SOL_AWC (available water capacity of the soil layer) (Table 2). In Table 4, the calibration parameters are placed in the order of the daily streamflow simulation sensitivity to them. This study selected a parameter set that provided the largest Nash-Sutcliffe model Efficiency coefficient (NSE) value among the ones that were identified as providing acceptable performance statistics (NSE greater than 0.5 and PBIAS smaller than ± 15%) in the model calibration (Table 4). Then, the chosen parameter set was incorporated into the SWAT model for a representative watershed for the following scenario analysis.

The differential split calibration and evaluation strategy (FCT and SCT) was employed to improve the representativity of a calibrated model (Table 5). The differences between performance statistics including NSEs, KGEs, and PBIASs obtained from FCT and SCT were not significant, but PBIAS values showed that parameter sets identified from SCT consistently overestimated the total flow volume in the calibration period but underestimated it in the evaluation period, but their sizes (less than 12%) were within the acceptable ranges.

An outlier was identified during the calibration period (Fig. A1a). The outlier could be explained by the uncertainty and errors in the rainfall data that were used for model calibration and evaluation. The total amount of rainfall reported on October 15, 2018 and October 16,

Table 6
Simulated responses of streamflow hydrograph components to the land cover change scenarios.

Afforestation scenarios								
Month	Total Water Yield (%)[a]				Baseflow (%)			
	A25	A50	A75	A100	A25	A50	A75	A100
Dec	1.9	3.7	5.3	6.8	1.9	3.7	5.3	6.8
Jan	2.3	4.3	6.6	8.6	2.3	4.3	6.6	8.6
Feb	1.8	3.6	5.4	7.2	1.8	3.6	5.4	7.2
Mar	1.5	3.1	5.2	6.7	1.5	3.1	5.2	6.7
Deforestation scenarios								
Month	Total Water Yield (%)				Baseflow (%)			
	D25	D50	D75	D100	D25	D50	D75	D100
Dec	-6.2	-12.2	-18.3	-24.0	-6.2	-12.2	-18.3	-24.0
Jan	-7.6	-15.1	-23.4	-30.9	-7.6	-15.1	-23.4	-30.9
Feb	-5.4	-9.9	-14.4	-18.0	-6.8	-13.1	-20.7	-27.0
Mar	-6.2	-12.4	-18.6	-24.7	-6.2	-12.4	-18.6	-24.7

[a] The numbers represent the amount of relative change from the baseline to a scenario: $relative\ change = (scenario - baseline)/baseline$

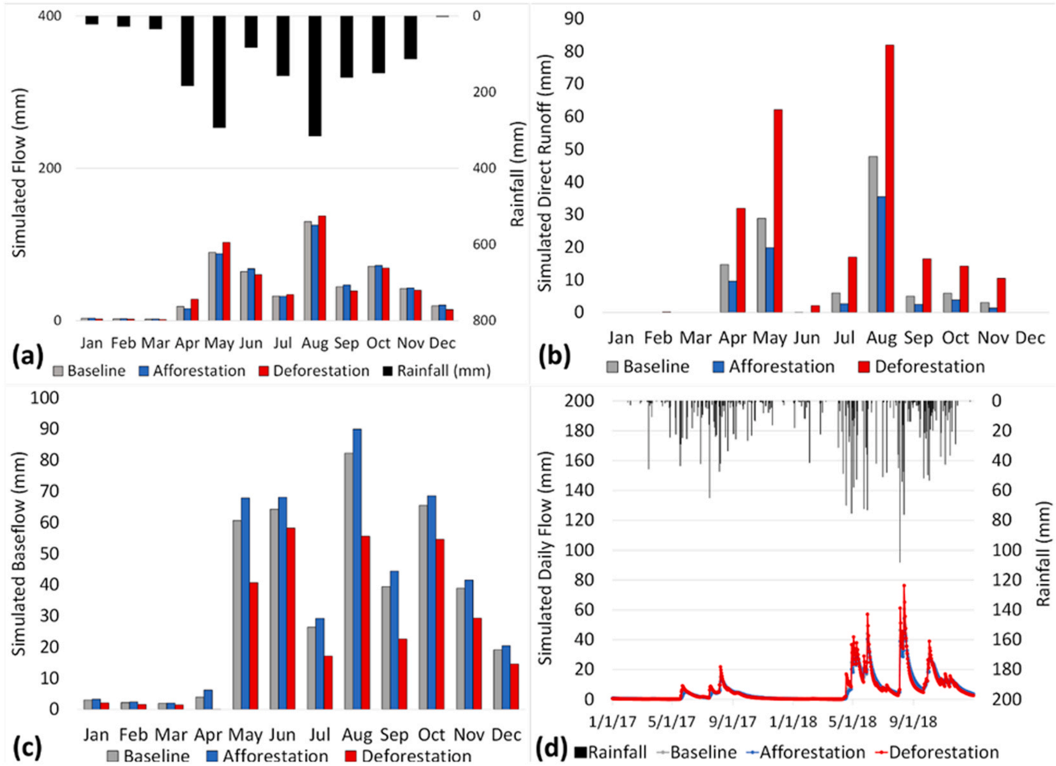

Fig. 7. Comparison of the temporal variability in streamflow (total runoff) simulated with SWAT for the land cover change scenario at the 100% coverage: flow (a), direct runoff (b) baseflow (c), and daily flow (d).

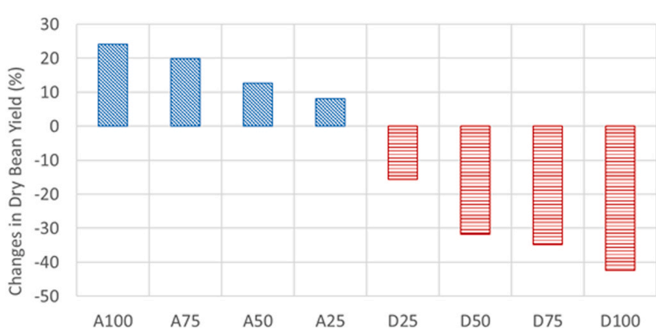

Fig. 8. Comparison of the yield variability simulated with the CSM–CROPGRO-Drybean model for each land use scenario.

2018 was 0 mm according to the UHM, but high flow discharges of 7.58 $cm^3\ s^{-1}$ and 8.02 $cm^3\ s^{-1}$ were observed for these two days. The recorded cumulative rainfall from 10/02/2018–10/16/2018 was 136 mm, and the total observed flow was 84 mm for the same period. The runoff ratio of 0.62 ($= 84\text{mm}/136\text{mm}$) seems reasonable when considering that October is in the middle of a wet season. Such comparisons between the rainfall records and the runoff observations demonstrated that rainfall observations from a single station might not be representative of the overall rainfall in a watershed due the spatial variability, especially in mountainous areas. The local rainfall data could not capture the timing of a rainfall event, even though it might be able to show the overall amount of long-term rainfall. Additionally, the local weather station is located approximately 10–13 km from the watershed. Thus, the spatial variability in rainfall in the region could lead to additional uncertainty in the rainfall data that were used for model calibration and evaluation. Despite this uncertainty, the model was able to simulate the large variability in the observed flow, except for the flow observed on October 16, 2018 (Fig. A1b).

The parameter sets calibrated to one (Wet2-Dry1) of the two pairs of wet and dry periods consistently provided higher NSE and lower KGE values, compared to ones calibrated to the other (Wet1-Dry2) (Table 5). Such calibration results indicate that, even though both objective functions are known to be sensitive to large values, KGE is more responsive to small values such as baseflow between storm events than NSE, as designed (Gupta et al., 2009). The results also indicate that the model relatively accurately predicted direct runoff or high flow during the Wet2-Dry1 period than during the other period (Table 5 and Fig. A1). For both periods, the baseflow was relatively accurately simulated by the model compared to the high flow. Overall, model performance was acceptable in simulating the daily water discharge of CRW in terms of NSE, R^2, and PBIAS (Table 5; Ritter and Muñoz-Carpena, 2013; Moriasi et al., 2015).

3.3. Streamflow impact analysis

The deforestation scenarios increased direct runoff by 30–113% and decreased baseflow by 7–28% on an annual basis depending on the size of the changes compared to the baseline (W25 to W100; Table 6 and Fig. 7). The changes in direct runoff and baseflow were canceled out to each other so that the total water yield did not change substantially (0.7–2%). However, for the afforestation scenarios, direct runoff decreased by 9–32%, while baseflow increased by 2–9%. The

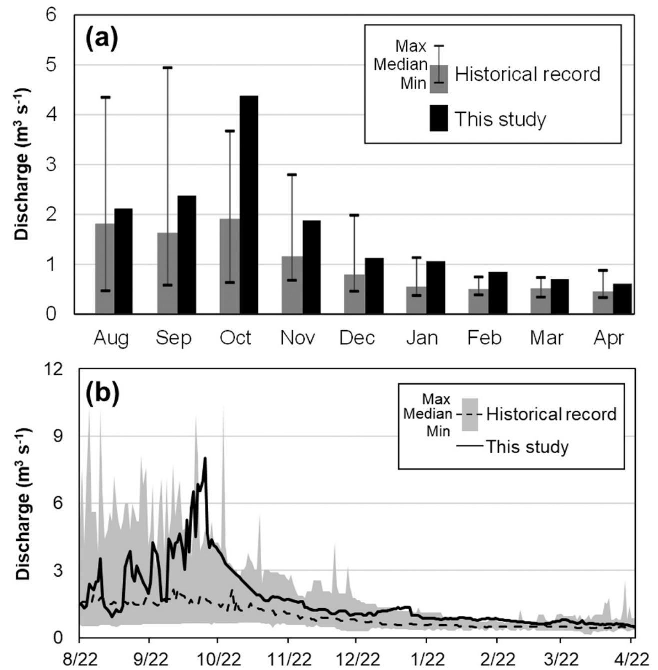

Fig. 9. Comparison of the seasonal streamflow variation observed in the two different periods, the current (2018–2019) and historical (1923–1939) periods. a) monthly and b) daily.

afforestation scenario also decreased the flow variability and increased the flow stability. As a result, the flashiness index decreased from 0.05 to 0.04 in 2017 and 0.1–0.08 in 2018 (Fig. 7). The total water yield did not change substantially; it only increased by 0.1% at an annual scale, compared to the current condition, but it increased by 2–8% during the dry season from December to March. Such results are attributed to the fact that the baseflow accounts for approximately 70% of the total streamflow in the study area. In contrast, for the deforestation scenario, the water yield decreased by 6–24% during the dry season. These findings are supported by previous studies that have related land use change to changes in direct runoff and baseflow (Belmar et al., 2016; Gashaw et al., 2017, 2018).

3.4. Dry bean yield impact analysis

The simulated streamflow discharges by SWAT for the dry bean growing season from December to March were incorporated into the CSM-CROPGRO-Drybean model to determine the impact of the land cover change scenarios on dry bean yield through the changes in streamflow that are available for irrigation for crop production. The crop modeling scenarios showed that the deforestation scenarios decreased the amount of available water from 6% to 25% (from W25 to W100) and, thus, resulted in a decrease in dry bean yield that ranged from 16% to 42% (Fig. 8). On the other hand, the afforestation scenarios increased dry bean yield by 8–24% by increasing the amount of water available for irrigation during the dry period from 2% to 7% (from A25 to A100; Table 6). These results demonstrate that water availability for irrigation is critical to crop production in the study area, suggesting that watershed land use management can improve crop production by helping to secure irrigation water.

Given the irrigation management practices of the region, the farmers collect water from the Courjolle River to irrigate the fields by surface irrigation. Dry bean yield followed a similar trend with the water availability during the growing season for each watershed condition. The reduction in the tree cover of the CRW, e.g., the deforestation scenarios, created a reduction in the amount of water available for irrigation from 6% to 25% compared to the baseline scenario. On the other hand, the afforestation scenarios increased the amount of water available for irrigation from 2% to 6%. As there is no reservoir in the irrigation district to store rainwater during the wet period, the land cover directly controls the availability of water for irrigation during the dry season.

4. Discussion

The watershed model was calibrated to observed daily streamflow, and sixteen parameters were selected for the calibration based on a knowledge of the parameters and streamflow sensitivity to them in the study watershed. In the sensitivity analysis, parameters related to the groundwater processes were identified as critical, which corresponds to the fact that approximately 70% of the total streamflow is contributed by baseflow. During model calibration, the curve numbers (CN2) were substantially reduced (by 25%) to allow the soil layers and shallow aquifer to quickly replenish soil water and groundwater during rainfall events. A long groundwater discharge delay time (18.2 days of GW_DELAY) and a low groundwater "revap" coefficient (0.03 of GW_REVAP) that were identified during calibration confirm that the groundwater processes have a dominant role in the hydrology of the watershed. The importance of groundwater should create more interest in developing forestation programs for the study areas since the afforestation scenario would generate more baseflow (more stable than direct runoff) and thus increase water availability, especially during the dry season. Such findings suggest the effectiveness of afforestation efforts for Haitian water resources and agriculture.

Data quantity and quality are two big challenges in model preparation, especially for study areas in developing countries. A limited amount of streamflow data did not allow for a comprehensive study on the applicability of the watershed model and reducing its uncertainty. This study could not continue the streamflow monitoring due to the safety and security conditions of the study areas. Because the study focuses on the growing season of dry bean, from December to March, in the study area located in Haiti; thus, the streamflow records collected for the limited time period might still be useful and valuable to this study. We tried to ensure the reliability of the monitoring data by comparing them with historical flow discharge records made by the Ministry of Agriculture (Ministère de l'Agriculture des Resources Naturelles et du Développement Rural: MARNDR) of Haiti from 1923 to 1939. The data were provided by the Unité Hydrométéorologique D'Haïti of MARNDR in 2018. From the comparison, we found that our streamflow monitoring data have greater seasonal (or monthly) variations compared to the historical records, implying a greater direct runoff contribution to the streamflow in recent years (Fig. 9). For example, the differences between the average daily streamflow discharge in October (the wettest month) and March (the driest month) were 3.68 cms and 1.53 cms for the current (2018–2019) and historical (1923–1939) periods, respectively. The relatively large direct runoff contribution to streamflow and the resulting large temporal streamflow variation (difference between streamflow discharges in the wettest and driest months) might be attributed to the deforestation processes that had occurred since the time when the historical flow measurements were made. At a daily scale, moreover, the variations of our flow monitoring data were generally covered by those of the historical records, but the streamflow discharges observed in the current periods (2018–2019) sometimes exceeded the historical maximum average daily flow in September and October (wet seasons; Fig. 9b). We could not find quantitative land cover data that can confirm this speculation that deforestation has progressed since the 1920s, but the literature reported that the land uses of Haiti had changed substantially from 1900 to 1961 and even after the period (e.g., 1980′s; Palmer, 1976; Hedges et al., 2018), which could explain the differences between the temporal streamflow variations observed in the current and historical periods. The comparison between the current and historical streamflow monitoring records provided an idea of how the hydrology of the drainage watershed has changed in the past 100 years.

The study areas are characterized by mountains and hills, which are known to increase the spatial variability of rainfall (Buytaert et al., 2006; Stefanidis and Stathis, 2018). The rainfall data were collected from a single weather station located at a distance of 13 km from the watershed, and the characteristics of orographic precipitation that is common in a mountainous watershed such as CRW might not be precisely captured by the station data. Other weather variables, including solar radiation, wind speed, relative humidity, minimum and maximum temperature were not available from the station; thus, they were retrieved from satellite-based estimates such as the NASA Power project database, which may include much uncertainty due to the spatial resolution (Stackhouse et al., 2018; White et al., 2008). The limited quantity of quality data and observations prevented this study from fully investigating the uncertainty of the modeling experiments, highlighting the role of field monitoring and measurements and suggesting a long-term investment in obtaining fundamental data, especially for developing countries.

The most recent official land cover data that were available for the study areas were prepared in 1998. Since then, changes might have happened in the watershed. Also, the definition of "savanna" can be different in terms of the densities and proportions of trees and grasses. A land cover type can be difficult to define quantitatively and precisely. For instance, "savanna" of the SWAT database may not be the same as that of CNIGS. We assumed that the boundary and quality of "savanna" that cover the majority (97%) of the study watershed did not change during the simulation period, which might have introduced additional uncertainty during watershed modeling and scenario analysis. In this study, we tried to verify this assumption by comparing the land use layer with the Google Map image and photos taken during field visits (made from August 20–24, 2018) and found that the savanna is still dominant in the study watershed (Fig. 1(b) and (c)).

The soil data used in the modeling experiment was derived from a global-scale soil database, FAO-UNESCO (FAO, 2003), which was prepared at a coarse resolution (1:5,000,000). Thus, it may not precisely represent the actual conditions of local soils and their spatial variations at the watershed scale, which might have added additional uncertainty to the modeling. Such epistemic uncertainty sources, including limited quantity and quality of observations, the lack of local rainfall observations, the categorical vagueness, and scale issues, would have affected the results of the modeling experiments. However, we left the uncertainty issue for future studies and focused on estimating the "relative" potential impact of the land use changes on the water availability and dry bean yield of the study areas.

This study tried to accurately represent agricultural management practices implemented in the downstream irrigation districts in the crop modeling based on the best of knowledge and information available for the study areas. However, several assumptions were required due to a lack of data and information. For instance, we assumed that local growers plant dry bean at the density recommended by the Ministry of Agriculture of Haiti, but not all the farmers may follow the recommendation. Diseases and insects can negatively affect crop growth and yield, which was not considered in the modeling. Fertilizers were assumed not to be restricted so that growers could apply fertilizers enough not to limit dry bean growth. Local farmers may grow several dry bean cultivars that may have different yield potential, and only some of them may be available to the farmers in specific years. We selected a dry bean cultivar that is the most common one (X-RAV-40, Mompremier et al., 2021), for which experimental data was available for the crop growth and yield calibration. Streamwater collected by the Courjolle River dam located at the outlet of CRW is diverted into two lined canals passing the irrigation districts and then distributed to individual dry bean fields through the earthen canal networks (Mompremier et al., 2021). The water diversion and distribution are determined by a local committee called the Association des Irrigants de la Plaine de l′Arcahaie (AIPA) mainly based on water availability, fees paid for the right to use the water, and field sizes. In reality, however, growers who have fields closer to the irrigation dam and canals want to get more water than the other growers with fields located relatively downstream of the dam, which created a great challenge for irrigation management. In this study, it was assumed that the same depth of irrigation water would be distributed to individual dry bean fields regardless of the proximity to the dam and canal and where the water use fees were paid or not. These assumptions might create biases in the crop yield and land cover impact estimates, probably overestimation.

The afforestation scenario increased total water yield and reduced direct runoff, which corresponds to other studies that reported the forest coverage could improve infiltration capacity, facilitate groundwater recharge, and then increase water availability during the dry season (Ilstedt et al., 2016a, 2016b; Filoso et al., 2017). The finding is also supported by the previous studies that investigated the interactions between land use and hydrological changes (Wilk and Hughes, 2002; Zhang et al., 2012; Neupane et al., 2015; Marhaento et al., 2017). The deforestation scenario increased direct runoff, on average, by 113% during the two years of simulation but decreased total water yield in the dry bean growing season (or dry period) between December and March. On the other hand, baseflow and total water yield increased during the dry period under the afforestation scenario. Similar results have been found in other studies (Sun et al., 2005; Belmar et al., 2016; Gashaw et al., 2017) that showed that the forest areas had a stabilization effect on the flow regime by increasing baseflow. Gebremicael et al. (2019) also found that forested or vegetated areas decreased wet-season flow and increased dry-season flow while bare land areas resulted in the opposite. The finding from this study provided additional evidence for a close linkage between watershed management and agricultural productivity and the effects of afforestation on water resources and agriculture.

Past studies that have been conducted in Haiti did not show the connection between crop yield and land use changes. In this context, there was a need to identify models that could assist with the simulation of both the hydrological processes and crop growth and yield prediction. The two models were selected to estimate the dry bean responses to land use scenarios. Coupling the two models, i.e., SWAT and CSM-CROPGRO-Drybean, was useful in the essence that the hydrologic model enabled the simulation of streamflow available from the watershed system, while the CSM-CROPGRO-Drybean model allowed the integration of the different amounts of water available from land use change scenarios that were simulated by the SWAT model and to estimate the responses of dry bean yield to these changes. In the end, coupling the two models for this study allowed exploring the linkage between crop yield and land use changes, i.e., afforestation and deforestation, which provides strategic insights for management practices. The information and data that were created in this study are expected to help decision-makers to develop efficient natural resource management plans and practices in Haiti.

5. Conclusion

Afforestation could help secure stable water resources and thus improve crop production in the study areas. On the other hand, deforestation made the watershed and agricultural areas vulnerable to drought by decreasing streamflow, especially baseflow in dry or growing seasons, and increasing its variability. The land use scenario of afforestation for the entire upstream drainage areas provided the largest water availability and crop production potential in the downstream irrigation district. Even the least afforestation scenario (25% of the upstream areas are afforested) could increase dry bean yield by 8% from increasing baseflow by 2% in the dry growing season. These results highlight the interconnection between the natural environment and agroecosystem and the importance of watershed and forest planning and management for improved agricultural sustainability. The afforestation scenarios could effectively manage both the water and agricultural resources. The scenario analysis results suggest that at least the current land use condition should be maintained to avoid a severe negative impact on crop production.

Declaration of Competing Interest

The authors declare that they have no known competing financial interests or personal relationships that could have appeared to influence the work reported in this paper.

Acknowledgment

This study was supported by a grant from the United States Agency for International Development (USAID) under the cooperative agreement # AID-OAA-A-15–00039. The contents are the responsibility of the authors and do not necessarily reflect the views of USAID or the United States Government. The authors acknowledge the support of Agronomist Alexander Gerry Delphin Leveille from the Unité Hydro Météorologique (UHM) of Haiti for providing the local weather data for the Arcahaie region.

Appendix A

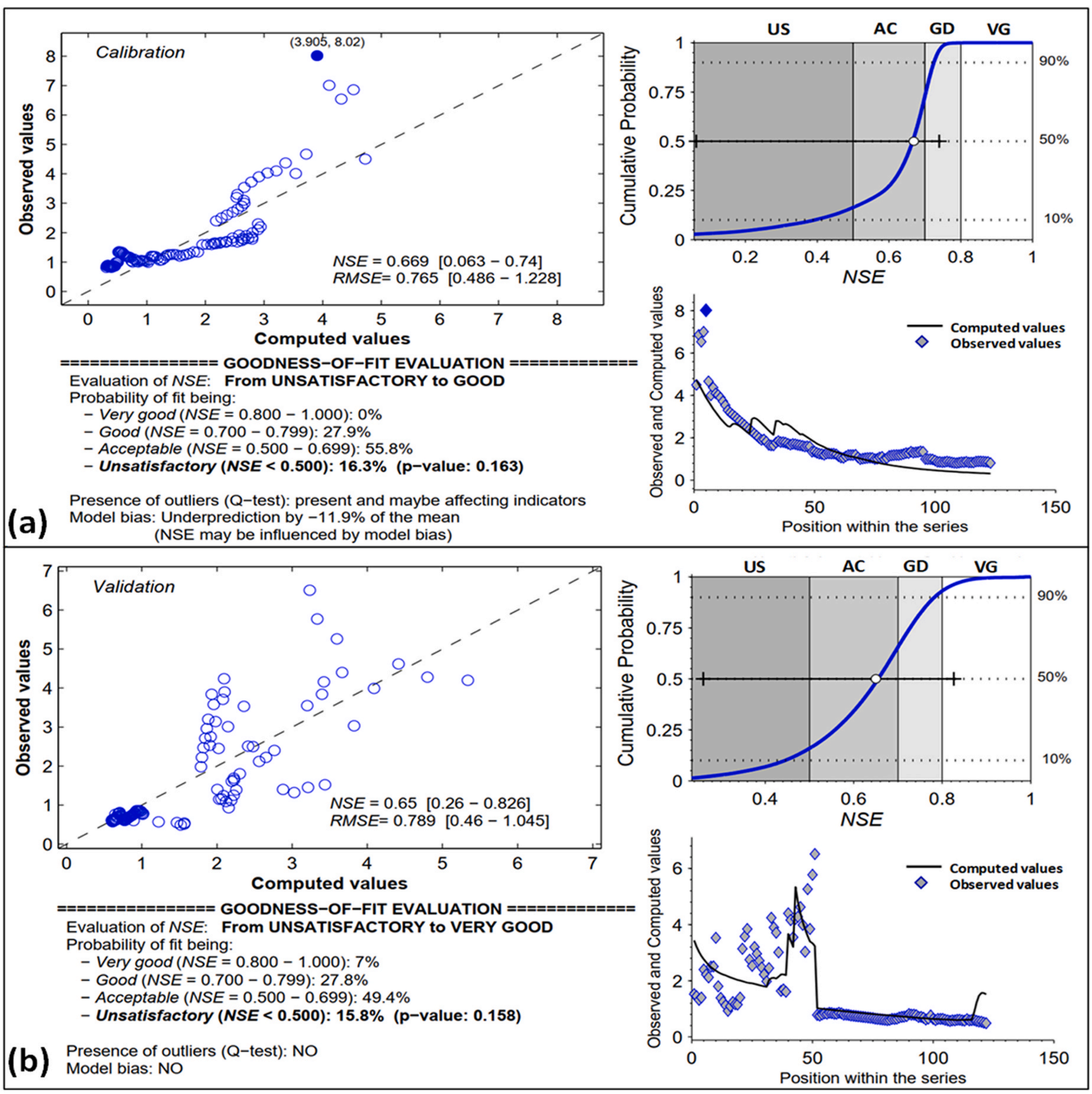

Fig. A1. SWAT model evaluations using the FITEVAL package; calibration period (a) and evaluation period (b). Observed and computed values are in m3s-1, NSE: Nash-Sutcliffe Efficiency, RMSE: Root Mean Square Error, US: unsatisfactory, AC: acceptable, GD: good, and VG: very good.

References

Abbaspour, K.C., Rouholahnejad, E., Vaghefi, S., Srinivasan, R., Yang, H., & Kløve, B., 2015, A continental-scale hydrology and water quality model for europe: Calibration and uncertainty of a high-resolution large-scale SWAT model doi://doi.org/10.1016/j.jhydrol.2015.03.027.

Abdelwahab, O.M.M., Bingner, R.L., Milillo, F., Gentile, F., 2014. Effectiveness of alternative management scenarios on the sediment load in a mediterranean agricultural watershed. J. Agric. Eng. 45 (3), 125–136. https://doi.org/10.4081/jae.2014.430.

Abdelwahab, O.M.M., Ricci, G.F., De Girolamo, A.M., Gentile, F., 2018. Modelling soil erosion in a mediterranean watershed: Comparison between SWAT and AnnAGNPS models. Environ. Res. 166, 363–376. https://doi.org/10.1016/j.envres.2018.06.029.

Anaba, L.A., Banadda, N., Kiggundu, N., Wanyama, J., Engel, B., Moriasi, D., 2017. Application of SWAT to assess the effects of land use change in the murchison bay catchment in uganda. Comput. Water, Energy, Environ. Eng. 6 (1), 24–40. https://doi.org/10.4236/cweee.2017.61003.

Arnold, J.G., Allen, P.M., 1999. Automated methods for estimating baseflow and ground water recharge from streamflow records. JAWRA J. Am. Water Resour. Assoc. 35 (2), 411–424. https://doi.org/10.1111/j.1752-1688.1999.tb03599.x.

Arnold, J.G., Allen, P.M., Muttiah, R., Bernhardt, G., 1995. Automated base flow separation and recession analysis techniques. Ground Water 33 (6), 1010–1018. https://doi.org/10.1111/j.1745-6584.1995.tb00046.x.

Arnold, J.G., Moriasi, D.N., Gassman, P.W., Abbaspour, K.C., White, M.J., Srinivasan, R., Jha, M.K., 2012. SWAT: model use, calibration, and validation. Trans. ASABE 55 (4), 1491–1508. https://doi.org/10.13031/2013.42256.

Arnold, J.G., Srinivasan, R., Muttiah, R.S., Williams, J.R., 1998. Large area hydrologic modeling and assessment part I: model development. J. Am. Water Resour. Assoc. 34 (1), 73–89. https://doi.org/10.1111/j.1752-1688.1998.tb05961.x.

Attia, A., Rajan, N., Xue, Q., Nair, S., Ibrahim, A., Hays, D., 2016. Application of DSSAT-CERES-Wheat model to simulate winter wheat response to irrigation management in the Texas High Plains. Agric. Water Manag. 165, 50–60.

Baker, D.B., Richards, R.P., Loftus, T.T., Kramer, J.W., 2004. A new flashiness index: Characteristics and applications to midwestern rivers and streams. J. Am. Water Resour. Assoc. 40 (2), 503–522.

Balogun Mohammed, A., Vijlee, S., Belmont, E., 2018. Technoeconomic feasibility of a sustainable charcoal industry to reduce deforestation in haiti. Sustain. Energy Technol. Assess. 29, 131–138. https://doi.org/10.1016/j.seta.2018.08.001.

Belmar, O., Barquín, J., Álvarez-Martínez, J.M., Peñas, F.J., Del Jesus, M., 2016. The role of forest maturity on catchment hydrologic stability. Hydrol. Earth Syst. Sci. Discuss. 1–17. https://doi.org/10.5194/hess-2016-471.

Bisantino, T., Bingner, R., Chouaib, W., Gentile, F., Trisorio Liuzzi, G., 2015. Estimation of runoff, peak discharge and sediment load at the event scale in a Medium-Size mediterranean watershed using the annagnps model. Land Degrad. Dev. 26 (4), 340–355. https://doi.org/10.1002/ldr.2213.

Bruijnzeel, L.A., 2004. Hydrological functions of tropical forest: Not seeing the soil for the trees? Agric., Ecosyst. Environ. 104 (104), 185–227 (Retrieved from). ⟨https://www.narcis.nl/publication/RecordID/oai:research.vu.nl:publications%2F738752a1-4d1a-48be-8c53-99eef8e06a85⟩.

Buytaert, W., Celleri, R., Willems, P., Bièvre, B.D., & Wyseure, G., 2006, Spatial and temporal rainfall variability in mountainous areas: a case study from the south ecuadorian andes. doi://doi.org/10.1016/j.jhydrol.2006.02.031.

Churches, C.E., Wampler, P.J., Sun, W., & Smith, A.J., 2014, Evaluation of forest cover estimates for haiti using supervised classification of landsat data. doi://doi.org/10.1016/j.jag.2014.01.020.

CNIGS, 2008, Land use land cover of haiti 1998. Port-au-Prince, Haiti: Haitian Centre for Geospatial Information.

CNSA/MARND, 2013, Evaluation prévisionnelle de la performance des récoltes de la campagne agricole de printemps 2013. Port-au-Prince, Haiti.

Dinku, T., Funk, C., Peterson, P., Maidment, R., Tadesse, T., Gadain, H., Ceccato, P., 2018. Validation of the CHIRPS satellite rainfall estimates over eastern africa. Q. J. R. Meteorol. Soc. 144 (S1), 292–312. https://doi.org/10.1002/qj.3244.

Dokoohaki, H., Gheysari, M., Mousavi, S.F., Hoogenboom, G., 2017. Effects of different irrigation regimes on soil moisture availability evaluated by CSM-CERES-Maize model under semi-arid condition. Ecohydrol. Hydrobiol. 17, 207–216. https://doi.org/10.1016/j.ecohyd.2017.06.001.

Dolisca, F., Carter, D.R., McDaniel, J.M., Shannon, D.A., Jolly, C.M., 2006a. Factors influencing farmers' participation in forestry management programs: a case study from haiti. For. Ecol. Manag. 236 (2), 324–331. https://doi.org/10.1016/j.foreco.2006.09.017.

Dolisca, F., Carter, D.R., McDaniel, J.M., Shannon, D.A., Jolly, C.M., 2006b. Factors influencing farmers' participation in forestry management programs: a case study from Haiti. For. Ecol. Manag. 236 (2–3), 324–331.

Dolisca, F., McDaniel, J.M., Shannon, D.A., Jolly, C.M., 2009. A multilevel analysis of the determinants of forest conservation behavior among farmers in haiti. Soc. Nat. Resour. 22 (5), 433–447. https://doi.org/10.1080/08941920802064448.

Dolisca, F., McDaniel, J.M., Teeter, L.D., 2007. Farmers' perceptions towards forests: a case study from haiti. For. Policy Econ. 9 (6), 704–712. https://doi.org/10.1016/j.forpol.2006.07.001.

FAO-UNESCO, 2003, Digital soil map of the world and derived soil properties [electronic resource] / FAO, UNESCO (Version 3.6 ed.). Rome: FAO.

Fews Net, & USAID, 2018, Haiti: Staple food market fundamentals, march 2018.FEWS NET. Retrieved from Business Premium Collection Retrieved from ⟨http://fews.net/sites/default/files/documents/reports/Haiti%20MFR_final_20180326.pdf⟩.

Ffolliott, P.F., Brooks, K.N., Fogel, M.M., 2002. Managing watersheds for sustaining agriculture and natural resource benefits into the future. Q. J. Int. Agric. 41 (1/2), 23–40 (Retrieved from). ⟨http://www.econis.eu/PPNSET?PPN=350311927⟩.

Filoso, S., Bezerra, M.O., Weiss, K.C.B., Palmer, M.A., 2017. Impacts of forest restoration on water yield: a systematic review. PLoS One 12 (8), e0183210. https://doi.org/10.1371/journal.pone.0183210.

Funk, C., Peterson, P., Landsfeld, M., Pedreros, D., Verdin, J., Shukla, S., Michaelsen, J., 2015. The climate hazards infrared precipitation with stations—a new environmental record for monitoring extremes. Sci. Data 2, 150066. https://doi.org/10.1038/sdata.2015.66.

Gardi, C., Angelini, M., Barceló, S., Comerma, J., Cruz Gaistardo, C., Encina Rojas, A., Vargas, R., 2014. *Atlas de suelos de américa latina y el caribe, comisión europea*. Oficina de Publicaciones de la Unión Europea, L-2995 Luxemburgo, Luxemburgo doi:10.2788/37334.

Gashaw, T., Tulu, T., Argaw, M., Worqlul, A., 2017. Evaluation and prediction of land use/land cover changes in the andassa watershed, blue nile basin, ethiopia. Environ. Syst. Res. 6 (1), 1–15. https://doi.org/10.1186/s40068-017-0094-5.

Gashaw, T., Tulu, T., Argaw, M., Worqlul, A.W., 2018. Modeling the hydrological impacts of land use/land cover changes in the andassa watershed, blue nile basin, ethiopia. Sci. Total Environ. 619–620, 1394–1408. https://doi.org/10.1016/j.scitotenv.2017.11.191.

Gassman, P.W., Reyes, M.R., Green, C.H., Arnold, J.G., 2007. The soil and water assessment tool: historical development, applications, and future research directions. Trans. ASABE 50 (4), 1211–1250. https://doi.org/10.13031/2013.23637.

Gebremicael, T.G., Mohamed, Y.A., & Van der Zaag, P., 2019, Attributing the hydrological impact of different land use types and their long-term dynamics through combining parsimonious hydrological modelling, alteration analysis and PLSR analysis doi://doi.org/10.1016/j.scitotenv.2019.01.085.

Germer, S., Neill, C., Vetter, T., Chaves, J., Krusche, A.V., Elsenbeer, H., 2009. Implications of long-term land-use change for the hydrology and solute budgets of small catchments in amazonia. J. Hydrol. 364 (3), 349–363. https://doi.org/10.1016/j.jhydrol.2008.11.013.

Ghilardi, A., Tarter, A., Bailis, R., 2018. Potential environmental benefits from woodfuel transitions in haiti: geospatial scenarios to 2027. Environ. Res. Lett. 13 (3), 35007. https://doi.org/10.1088/1748-9326/aaa846.

Giri, S., Qiu, Z., Prato, T., Luo, B., 2016. An integrated approach for targeting critical source areas to control nonpoint source pollution in watersheds. Water Resour. Manag. 30 (14), 5087–5100. https://doi.org/10.1007/s11269-016-1470-z.

Gupta, H.V., Kling, H., Yilmaz, K.K., & Martinez, G.F., 2009, Decomposition of the mean squared error and NSE performance criteria: Implications for improving hydrological modelling. doi://doi.org/10.1016/j.jhydrol.2009.08.003.

Haan, C.T., Barfield, B.J., Hayes, J.C., 1994. Design Hydrology and Sedimentology for Small Catchments. Elsevier.

Harmel, R.D., Baffaut, C., Douglas-Mankin, K.R., 2018. Review and development of ASABE engineering practice 621: "Guidelines for calibrating, validating, and evaluating hydrologic and water quality models". Trans. ASABE 61 (4), 1393–1401. https://doi.org/10.13031/trans.12806.

Hedges, S.B., Cohen, W.B., Timyan, J., Yang, Z., 2018. Haiti's biodiversity threatened by nearly complete loss of primary forest. Proc. Natl. Acad. Sci. U. S. A. 115 (46), 11850–11855.

Heinemann, A.B., Hoogenboom, G., Georgiev, G.A., De Faria, R.T., Frizzone, J.A., 2000. Center pivot irrigation management optimization of dry beans in humid areas. Trans. Am. Soc. Agric. Eng. https://doi.org/10.13031/2013.3050.

Her, Y., Chaubey, I., Frankenberger, J., Jeong, J., 2017. Implications of spatial and temporal variations in effects of conservation practices on water management strategies. Agric. Water Manag. 180, 252–266. https://doi.org/10.1016/j.agwat.2016.07.004.

Her, Y., Chaubey, I., Frankenberger, J., Smith, D., 2016. Effect of conservation practices implemented by USDA programs at field and watershed scales. J. Soil Water Conserv. 71 (3), 249–266. https://doi.org/10.2489/jswc.71.3.249.

Her, Y., Frankenberger, J., Chaubey, I., Srinivasan, R., 2015. Threshold effects in HRU definition ofthe soil and water assessment tool. Trans. ASABE 58 (2), 367–378. https://doi.org/10.13031/trans.58.10805.

Her, Y., Heatwole, C., 2016. Comparing impacts of parameter and spatial data uncertainty for a grid-based distributed watershed model. J. Hydroinf. 18 (6), 961–974. https://doi.org/10.2166/hydro.2016.003.

He, H., Zhou, J., Zhang, W., 2008. Modelling the impacts of environmental changes on hydrological regimes in the hei river watershed, china. Glob. Planet. Change 61 (3), 175–193. https://doi.org/10.1016/j.gloplacha.2007.08.012.

Hoogenboom, G.J.W., Jones, Boote, K.J., 1992. Modeling growth, development and yield of grain legumes using SOYGRO, PNUTGRO, and BEANGRO: a review. Trans. ASAE 35 (6), 2043–2056.

Hoogenboom, G., Porter, C.H., Boote, K.J., Shelia, V., Wilkens, P.W., Singh, U., White, J. W., Asseng, S., Lizaso, J.I., Moreno, L.P., Pavan, W., Ogoshi, R., Hunt, L.A., Tsuji, G. Y., Jones, J.W., 2019a. The DSSAT crop modeling ecosystem. In: Boote, K.J. (Ed.), Advances in Crop Modeling for a Sustainable Agriculture. Burleigh Dodds Science Publishing, Cambridge, United Kingdom, pp. 173–216. https://doi.org/10.19103/AS.2019.0061.10.

Hoogenboom, G., Porter, C.H., Shelia, V., Boote, K.J., Singh, U., White, J.W., Hunt, L.A., Ogoshi, R., Lizaso, J.I., Koo, J., Asseng, S., Singels, A., Moreno, L.P., and Jones, J.W., 2019b, Decision Support System for Agrotechnology Transfer (DSSAT) Version 4.7.5 (https://DSSAT.net). DSSAT Foundation, Gainesville, Florida, USA.

Hoogenboom, G., White, J.W., Jones, J.W., Boote, K.J., 1994. BEANGRO, a process oriented dry bean model with a versatile user interface. Agron. J. 86 (1), 182–190.

Huisman, J.A., Breuer, L., Bormann, H., Bronstert, A., Croke, B.F.W., Frede, H., Willems, P., 2009, Assessing the impact of land use change on hydrology by ensemble modeling (LUCHEM) III: Scenario analysis. doi://doi.org/10.1016/j.advwatres.2008.06.009.

Hundal, S.S., Prabhjyot-Kaur, 1997, Application of the CERES-Wheat model to yield predictions in the irrigated 260 J.W. Jones et al. / Europ. J. Agronomy 18 (2003) 235/265 plains of the Indian Punjab. Journal of Agricultural Science 129, 13/18.

Ilstedt, U., Bargués Tobella, A., Bazié, H.R., Bayala, J., Verbeeten, E., Nyberg, G., Malmer, A., 2016a. Intermediate tree cover can maximize groundwater recharge in the seasonally dry tropics. Sci. Rep. 6 (1), 21930. https://doi.org/10.1038/srep21930.

Ilstedt, U., Tobella, A.B., Bazié, H.R., Bayala, J., Verbeeten, E., Nyberg, G., Malmer, A., 2016b. Intermediate tree cover can maximize groundwater recharge in the seasonally dry tropics. Sci. Rep. 6 (1), 1–12.

Jeong, H., Jang, T., Seong, C., Park, S., 2014. Assessing nitrogen fertilizer rates and split applications using the DSSAT model for rice irrigated with urban wastewater. Agric. Water Manag. 141, 1–9.

Jeune, W., 2015, Solos e ambientes no haiti ocidental: Gênese, classificação e mapeamento. Retrieved from ⟨www.locus.ufv.br/handle/123456789/10345⟩.

Jones, J.W., Hoogenboom, G., Porter, C.H., Boote, K.J., Batchelor, W.D., Hunt, L.A., Wilkens, P.W., Singh, U., Gijsman, A.J., Ritchie, J.T., 2003. DSSAT cropping system model. Eur. J. Agron. 18, 235–265.

Van Liew, M.W., Veith, T.L., Bosch, D.D., Arnold, J.G., 2007. Suitability of SWAT for the conservation effects assessment project: comparison on USDA agricultural research service watersheds. J. Hydrol. Eng. 12 (2), 173–189.

Lopez, J.R., Winter, J.M., Elliott, J., Ruane, A.C., Porter, C., Hoogenboom, G., 2017. Integrating growth stage deficit irrigation into a process based crop model. Agric. For. Meteorol. 243, 84–92. https://doi.org/10.1016/j.agrformet.2017.05.001.

MacRobert, J.F., Savage, M.J., 1998. The use of a crop simulation model for planning wheat irrigation in Zimbabwe. In: Tsuji, G.Y., Hoogenboom, G., Thornton, P.K. (Eds.), Understanding Options for Agricultural Production. Kluwer Academic Publishers, Dordrecht, the Netherlands, 205/220.

Maldonado, W., Valeriano, T.T.B., & de Souza Rolim, G., 2019, EVAPO: A smartphone application to estimate potential evapotranspiration using cloud gridded meteorological data from NASA-POWER system. doi://doi.org/10.1016/j.compag.2018.10.032.

Malik, W., Isla, R., Dechmi, F., 2019. DSSAT-CERES-maize modelling to improve irrigation and nitrogen management practices under Mediterranean conditions. Agric. Water Manag. 213, 298–308. https://doi.org/10.1016/J.AGWAT.2018.10.022.

Malik, W., Jiménez-Aguirre, M.T., Dechmi, F., 2020. Coupled DSSAT-SWAT models to reduce off-site N pollution in Mediterranean irrigated watershed. Sci. Total Environ. 745. https://doi.org/10.1016/j.scitotenv.2020.141000.

Marhaento, H., Booij, M.J., Rientjes, T.H.M., Hoekstra, A.Y., 2017. Attribution of changes in the water balance of a tropical catchment to land use change using the SWAT model. Hydrol. Process. 31 (11), 2029–2040. https://doi.org/10.1002/hyp.11167.

MARNDR, 2012. Politique d'irrigation du MARNDR 2012-2016. Ministère de l'Agriculture des Ressources Naturelles et du Développement Rural, Port-au-Prince, Haiti.

McClintock, N.C., 2003, Agroforestry and sustainable resource conservation in haiti: a case study.

McKay, M.D., Beckman, R.J., Conover, W.J., 1979. A comparison of three methods for selecting values of input variables in the analysis of output from a computer code. Technometrics 21 (2), 239–245. https://doi.org/10.1080/00401706.1979.10489755.

McKay, M.D., Beckman, R.J., Conover, W.J., 2000. A comparison of three methods for selecting values of input variables in the analysis of output from a computer code. Technometrics 42 (1), 55–61. https://doi.org/10.1080/00401706.2000.10485979.

Molnar, J.J., Kokoye, S., Jolly, C., Shannon, D.A., Huluka, G., 2015. Agricultural development in northern haiti: Mechanisms and means for moving key crops forward in a changing climate. J. Agric. Environ. Sci. 4 (No. 2), 17. https://doi.org/10.15640/jaes.v4n2a4.

Mompremier, R., Her, Y., Hoogenboom, G., Migliaccio, K., Muñoz-Carpena, R., Brym, Z., Colbert, R.W., Jeune, W., 2021. Modeling the response of dry bean yield to irrigation water availability controlled by watershed hydrology. Agric. Water Manag. 243 (1), 106429 https://doi.org/10.1016/j.agwat.2020.106429.

Moriasi, D.N., Gitau, M.W., Pai, N., Daggupati, P., 2015. Hydrologic and water quality models: performance measures and evaluation criteria. Trans. ASABE 58 (6), 1763–1785. https://doi.org/10.13031/trans.58.10715.

Muñoz-Villers, L.E., McDonnell, J.J., 2013. Land use change effects on runoff generation in a humid tropical montane cloud forest region. Hydrol. Earth Syst. Sci. 17 (9), 3543–3560. https://doi.org/10.5194/hess-17-3543-2013.

Naef, F., Scherrer, S., & Weiler, M., 2002, A process based assessment of the potential to reduce flood runoff by land use change. doi://doi.org/10.1016/S0022–1694(02)00141–5.

Nash, J.E., Sutcliffe, J.V., 1970. River flow forecasting through conceptual models part I — a discussion of principles. J. Hydrol. 10 (3), 282–290. https://doi.org/10.1016/0022-1694(70)90255-6.

Neitsch, S.L., Arnold, J.G., Kiniry, J.R., & Williams, J.R., 2011, Soil and water assessment tool, theoretical documentation version 2009: TR-406. College Station, Texas 77843–2118: Texas Water Resources Institute. Retrieved from ⟨https://swat.tamu.edu/media/99192/swat2009-theory.pdf⟩.

Nepal, S., Flügel, W., Shrestha, A., 2014. Upstream-downstream linkages of hydrological processes in the himalayan region. Ecol. Process. 3 (1), 1–16. https://doi.org/10.1186/s13717-014-0019-4.

Neupane, R.P., White, J.D., Alexander, S.E., 2015. Projected hydrologic changes in monsoon-dominated himalaya mountain basins with changing climate and deforestation. J. Hydrol. 525, 216–230. https://doi.org/10.1016/j.jhydrol.2015.03.048.

Nicolas, F., Migliaccio, K.W., Hoogenboom, G., Rathinasabapathi, B.R., Eisenstadt, W.R., 2020. Assessing the potential impact of climate change on rice yield in the artibonite valley of haiti using the CSM-Ceres-Rice model. Trans. ASABE 63, 1385–1400. https://doi.org/10.13031/TRANS.13868.

Nikolaidis, N.P., Bouraoui, F., Bidoglio, G., 2013. Hydrologic and geochemical modeling of a karstic mediterranean watershed. J. Hydrol. 477, 129–138. https://doi.org/10.1016/j.jhydrol.2012.11.018.

Ben Nouna, B., Katerji, N., Mastrorilli, M., 2000. Using the CERES-Maize model in a semi-arid Mediterranean environment. Evaluation of model performance. Eur. J. Agron. 13, 309–322. https://doi.org/10.1016/S1161-0301(00)00063-0.

Palmer, E.C., 1976. Land use and Landscape Change Along the Dominican-Haitian Borderlands. University of Florida.

Pandey, A., Himanshu, S.K., Mishra, S.K., & Singh, V.P., 2016, Physically based soil erosion and sediment yield models revisited. doi://doi.org/10.1016/j.catena.2016.08.002.

Poff, N.L., Allan, J.D., Bain, M.B., Karr, J.R., Prestegaard, K.L., Richter, B.D., Stromberg, J.C., 1997. The natural flow regime. BioScience 47 (11), 769–784.

RGA/MARNDR, CNIGS, FAO & European Union, 2012, Atlas agricole d'haiti: Carte de prédominance géographique des monocultures: Spécilité culturale des communes. Retrieved from ⟨http://agriculture.gouv.ht/statistiques_agricoles/Atlas/utilisationParcelles.html⟩.

Ritter, A., & Muñoz-Carpena, R., 2013, Performance evaluation of hydrological models: statistical significance for reducing subjectivity in goodness-of-fit assessments. doi://doi.org/10.1016/j.jhydrol.2012.12.004.

Runge, C.F., White, T.A., 1994. Common property and collective action: Lessons from cooperative watershed management in haiti. Econ. Dev. Cult. Change 43 (1), 1–41 (Retrieved from). ⟨http://econpapers.repec.org/article/ucpecdecc/v_3a43_3ay_3a1994_3ai_3a1_3ap_3a1-41.htm⟩.

Sahin, V., Hall, M.J., 1996. The effects of afforestation and deforestation on water yields. J. Hydrol. 178 (1–4), 293–309.

Scheffler, R., Neill, C., Krusche, A.V., Elsenbeer, H., 2011. Soil hydraulic response to land-use change associated with the recent soybean expansion at the amazon agricultural frontier. Agric., Ecosyst. Environ. 144 (1), 281–289. https://doi.org/10.1016/j.agee.2011.08.016.

Schilling, K.E., Jha, M.K., Zhang, Y., Gassman, P.W., Wolter, C.F., 2008. Impact of land use and land cover change on the water balance of a large agricultural watershed: historical effects and future directions. Water Resour. Res. 44 (7) https://doi.org/10.1029/2007WR006644.

Siad, S.M., Iacobellis, V., Zdruli, P., Gioia, A., Stavi, I., Hoogenboom, G., 2019. A review of coupled hydrologic and crop growth models. Agric. Water Manag. 224 (229), 105746 https://doi.org/10.1016/j.agwat.2019.105746.

Stackhouse, P.W.J., Zhang, T., Westberg, D., Barnett, A.J., Bristow, T., Macpherson, B., & Hoell, J.M., 2018, POWER release 8.0.1 (with GIS applications) methodology (data parameters, sources, and validation).

Steele, D.D., Stegman, E.C., Knighton, R.E., 2000. Irrigation management for corn in the northern Great Plains, USA. Irrig. Sci. 19, 107–114. https://doi.org/10.1007/PL00006709.

Stefanidis, S., Stathis, D., 2018. Spatial and temporal rainfall variability over the mountainous central pindus (greece). Climate 6 (3), 75. https://doi.org/10.3390/cli6030075.

Sun, G., McNulty, S.G., Lu, J., Amatya, D.M., Liang, Y., Kolka, R.K., 2005. Regional annual water yield from forest lands and its response to potential deforestation across the southeastern united states. J. Hydrol. 308 (1), 258–268. https://doi.org/10.1016/j.jhydrol.2004.11.021.

Tarter, A., 2016. Charting charcoal in haiti. Anthropol. N. 57 (7), e71. https://doi.org/10.1111/AN.43.

Tarter, A., Freeman, K.K., Ward, C., Sander, K., Theus, K., Coello, B., Ahmed, T.T.G., 2017. Charcoal in Haiti: A National Assessment of Charcoal Production and Consumption Trends. World Bank, Washington, DC. ⟨http://hdl.handle.net/10986/31257⟩.

Thanapakpawin, P., Richey, J., Thomas, D., Rodda, S., Campbell, B., Logsdon, M., 2007. Effects of landuse change on the hydrologic regime of the mae chaem river basin, NW thailand. J. Hydrol. 334 (1), 215–230. https://doi.org/10.1016/j.jhydrol.2006.10.012.

USGS, 2019, USGS EROS Archive - Digital Elevation - Shuttle Radar Topography Mission (SRTM) 1 Arc-Second Global.

Wampler, P.J., Tarter, A., Bailis, R., Sander, K., Sun, W., 2019. Discussion of forest definitions and tree cover estimates for Haiti. Proc. Natl. Acad. Sci. U. S. A. 116 (12), 5202–5203.

White, J.W., Hoogenboom, G., Stackhouse, P.W., Hoell, J.M., 2008. Evaluation of NASA satellite- and assimilation model-derived long-term daily temperature data over the continental US. Agric. For. Meteorol. 148 (10), 1574–1584.

Widmer, J.M., Sergile, F., Cheremond, Y., Morris, J.G., 2018. VisiEAU 2018—a vision for water in Haiti, 2018. Emerg. Infect. Dis. 24 (10) https://doi.org/10.3201/eid2410.180693.

Wilk, J., Hughes, D.A., 2002. Simulating the impacts of land-use and climate change on water resource availability for a large south indian catchment. Hydrol. Sci. J. 47 (1), 19–30. https://doi.org/10.1080/02626660209492904.

Wohl, E., Barros, A., Brunsell, N., Chappell, N.A., Coe, M., Giambelluca, T., Ogden, F., 2012. The hydrology of the humid tropics. Nat. Clim. Change 2, 655–662. https://doi.org/10.1038/nclimate1556.

Yan, B., Fang, N.F., Zhang, P.C., Shi, Z.H., 2013. Impacts of land use change on watershed streamflow and sediment yield: An assessment using hydrologic modelling and partial least squares regression. J. Hydrol. 484, 26–37. https://doi.org/10.1016/j.jhydrol.2013.01.008.

Ye, K.Q., 1998. Orthogonal column latin hypercubes and their application in computer experiments. J. Am. Stat. Assoc. 93 (444), 1430–1439. https://doi.org/10.1080/01621459.1998.10473803.

Zhang, M., Wei, X., Sun, P., Liu, S., 2012. The effect of forest harvesting and climatic variability on runoff in a large watershed: the case study in the upper minjiang river of yangtze river basin. J. Hydrol. 464–465, 1–11. https://doi.org/10.1016/j.jhydrol.2012.05.050.